Molecular and mechanical characterization of reactive ethylene–propylene elastomers and their use in PA6-based blends

M. Abbate, V. Di Liello, E. Martuscelli, P. Musto, G. Ragosta and G. Scarinzi

Istituto di Ricerche su Tecnologia dei Polimeri e Reologia del C.N.R., Via Toiano 6, 80072 Arco Felice (NA), Italy

(Received 23 April 1991; accepted 25 June 1991)

The nature of the molecular interactions occurring in an ethylene–propylene copolymer functionalized by succinic anhydride groups has been investigated by using *FT*i.r. spectroscopy. Hydrogen bonding interactions between carboxylic acid units and between carboxylic acid and anhydride groups have been identified. The mechanical tensile properties of such modified elastomers have been investigated and interpreted in terms of the molecular interactions detected spectroscopically. Finally, the effectiveness of these functionalized rubbers as toughening agents for polyamide-6 has also been examined.

(Keywords: EPR copolymer; *FT*i.r. spectroscopy; mechanical properties; PA6)

INTRODUCTION

Ethylene–propylene (EPR) copolymers have been modified by attaching unsaturated polar groups onto their chain backbones in order to improve such properties as adhesion and dyeability or to perform successive reactions such as cross-linking or grafting. Functionalization has generally been achieved in solvent media and initiated by means of organic peroxides[1–4]. The most commonly used functional molecule has been maleic anhydride, owing to the high reactivity of the anhydride group in successive reactions. In fact such modified EPR copolymers (EPR-g-SA) have been used in polyamide-6 (PA6) and in poly(butadiene/terephthalate) (PBT) blends prepared either by melt mixing of the components or during the polymerization of the matrix monomers[5–7]. These blends succeeded in greatly improving the impact resistance of the thermoplastic matrix at low temperatures, especially those obtained by melt mixing. A molecular as well as a mechanical characterization of these modified EPRs appears to be interesting in order to evaluate their potential end uses.

In the present study the results of a Fourier transform infrared (*FT*i.r.) spectroscopic investigation and those from a tensile-mechanical analysis made on an EPR sample with 28 wt% C_3, modified by grafting different amounts of maleic anhydride through a solution process, are reported. The main aim of the study was to draw a correlation between the molecular interactions occurring within the material and its mechanical response. Furthermore, the effectiveness of such modified copolymers as toughening agents in PA6-based blends has been confirmed.

0032-3861/92/142940-09

EXPERIMENTAL

Materials

The EPR copolymer (tradename CTX 032) supplied by Dutral S.p.A. had an ethylene content of 78 mol%. EPR-g-SA with a grafting degree of 1.3, 3.0 and 4.4 wt% was prepared following the procedure already described elsewhere[2]. The PA6 used was a SNIAMID ASN27/S produced by SNIA viscosa, with $\bar{M}_n = 2.3 \times 10^4$. Before use the PA6 was kept under vacuum at 60°C for 48 h.

Blend preparation

Binary PA6/EPR and PA6/EPR-g-SA blends with a composition 80/20 by weight were prepared in a Brabender-like apparatus (Rheocord E.C. of Haake Inc.) at a temperature of 260°C for a mixing time of 20 min and at a roller speed of 32 rev min^{-1}.

Techniques

*FT*i.r. measurements were made on thin films (ca. 10 μm) with a Nicolet 5DX-B spectrometer equipped with a deuterated triglicyne sulphate (DTGS) detector and a germanium on KBr beam-splitter. The scanned wavenumber range was 4000–400 cm^{-1} at a resolution of 2 cm^{-1}. The frequency scale was internally calibrated to an accuracy of 0.02 cm^{-1} by a He/Ne reference laser. The interferograms were Fourier transformed by using a Happ–Ganzel apodization function. The temperature measurements were made in a SPECAC temperature cell directly mounted in the spectrometer. This unit was driven by a Eurotherm 071 temperature controller to an accuracy of ± 1°C.

Tensile tests were made with an Instron machine (Model 1122) at ambient temperature and at a cross-head speed of 5 mm min^{-1}. The dumb-bell-shaped specimens used were cut from sheets obtained by compression moulding. Before testing, the blend specimens were conditioned in hot water at 90°C in order to obtain the same amount of absorbed water (about 3 wt%). The exact procedure is reported in a previous contribution[5].

Charpy impact tests were made at an impact speed of 1 m s^{-1} by using an instrumented CEAST pendulum. Samples sharply notched were fractured at different temperatures ranging from −60 to 20°C. The temperature was changed by means of a liquid-nitrogen home-made apparatus. Before testing, the specimens were dried under vacuum at 90°C for 10 h.

Cryogenically fractured surfaces of PA6/EPR blends were exposed for 30 min to boiling xylene vapours and subsequently examined by a scanning electron microscope (Philips SEM 501). SEM examination was also performed on Charpy fractured surfaces not subjected to the etching treatment.

RESULTS AND DISCUSSION

Characterization of the functionalized rubbers

Spectroscopic analysis. The *FT*i.r. spectra in the range 4000–400 cm^{-1} of the plain EPR and of the EPR-g-SA having a grafting degree of 3.0 wt% are reported in *Figure 1*, curves A and B, respectively.

The spectrum of plain EPR shows, in addition to the very intense ν_{CH} vibrations in the range 3000–2750 cm^{-1}, the characteristic pattern of saturated polyolefins. In particular the hydrogen bending vibrations of the CH_2 groups and the asymmetrical CH_3 deformation overlap into an intense absorption approximately centred at 1460 cm^{-1}, while the symmetrical CH_3 bending mode is responsible for the sharp peak at 1377 cm^{-1}. A weak absorption near 1300 cm^{-1} has been attributed to a CH_2 wagging mode. Finally, at 721 cm^{-1} occurs the characteristic band arising from the rocking mode of the structure $(CH_2)_n$ with $n \geqslant 4$. The spectrum of the functionalized rubber (*Figure 1*, curve B) clearly shows the peaks arising from the grafted succinic anhydride units. In particular, at 1863 cm^{-1} and at 1785 cm^{-1} are observed the peaks attributed to the symmetric and asymmetric stretching vibration of the anhydride carbonyls, respectively[8,9]. In this region a weaker absorption centred at 1712 cm^{-1} is also found. Such a peak is assigned to succinic acid functionalities formed in low concentration during the grafting process and/or during the film preparation procedure, by hydrolysis of anhydride groups. From the position of this stretching mode it is possible to conclude that, even when the concentration of succinic acid groups is very low (below 0.35 wt%), they are still able to partially self-associate through strong hydrogen-bonding interactions. In fact the $\nu_{C=O}$ absorption of 'free' COOH groups would lie at a frequency about 30 cm^{-1} higher than the one observed.

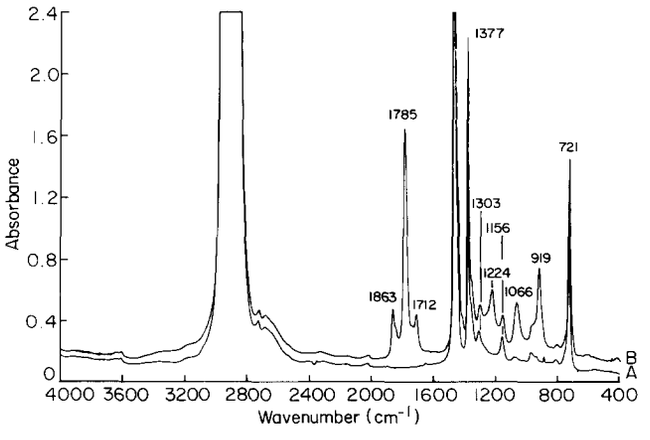

Figure 1 *FT*i.r. spectra in the range 4000–400 cm^{-1} of pure EPR (A) and EPR-g-SA with a grafting degree of 3.0 wt% (B)

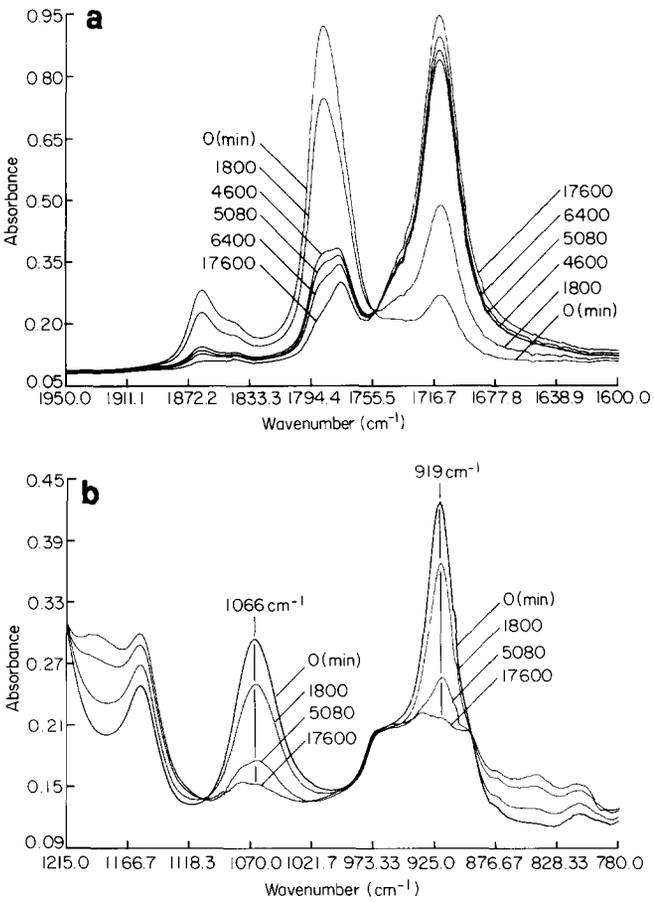

Figure 2 *FT*i.r. spectra in the range 1950–1600 cm^{-1} (A) and in the range 1215–780 cm^{-1} (B) of EPR-g-SA hydrolysed at room temperature for different time periods: hydrolysis times as indicated (all the spectra are reported in absolute absorbance scale)

In the fingerprint region three more peaks characteristic of the cyclic anhydride structure are identified at 1224 cm^{-1} (–C–O–C– stretching mode) at 1066 cm^{-1} and at 919 cm^{-1}. In particular, the band at 1066 cm^{-1} is highly symmetrical and is practically free from any interfering EPR absorption. For such reasons it appears to be particularly well suited for quantitative determinations. The anhydride functionalities grafted onto the EPR backbone are very prone to undergo hydrolysis even at room temperature. A quantitative evaluation of the hydrolysis rate at 25°C and at a relative humidity of 50 ± 2% has been achieved by following the variation of the complex carbonyl region of the spectrum with exposure time. The spectra collected at various times in the range 1990–1590 cm^{-1} are reported in *Figure 2*. The increase with time of the carboxylic absorption at 1712 cm^{-1} and the corresponding decrease of the anhydride doublet at 1863 and 1785 cm^{-1} is evident.

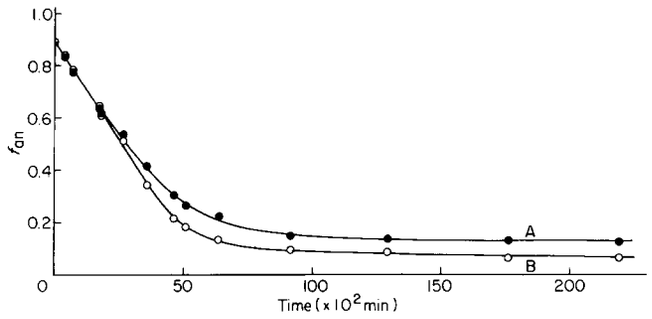

Figure 3 Fraction of anhydride groups (f_{an}) as a function of hydrolysis time: (●) determination obtained from the carbonyl peaks; (○) determination obtained from the 1066 cm^{-1} peak

The anhydride peak at 1785 cm^{-1} also shows the gradual development of a finer structure. This feature will be discussed in more detail later.

From literature data on infrared spectroscopy of ethylene–maleic-anhydride copolymers[10], it was found that the integral molar absorptivity of anhydride groups ε_{an}, defined as

$$\varepsilon_{an} = \frac{\bar{A}_{an}}{l[An]}$$

where

$$\bar{A}_{an} = \int_{1770}^{1923} A \, dv$$

l is the sample thickness and [An] is the anhydride group concentration, which is equal to 2.15×10^4 l mol^{-1} cm^{-2}. Moreover, the integral molar absorptivity of the succinic acid functionalities, ε_{ac}, defined in the same way, but where

$$\bar{A}_{ac} = \int_{1667}^{1770} A \, dv$$

was found to be 2.19×10^4 l mol^{-1} cm^{-2}.

On the basis of the ratio $\varepsilon_{an}/\varepsilon_{ac} = 0.982$, the fraction of anhydride groups, $f_{an} = [An]/\{[An] + [Ac]\}$ can be calculated from the total area of the carbonyl absorption according to the relation:

$$f_{an} = \frac{\bar{A}_{an}}{\bar{A}_{an} + (\varepsilon_{an}/\varepsilon_{ac})/\bar{A}_{ac}}$$

In *Figure 3*, curve A, f_{an} is reported as a function of exposure time. It is observed that the hydrolysis of anhydride groups proceeds at a constant rate of 1.56×10^{-4} min^{-1} up to approximately 5000 min. The conversion at the end of this period is about 75%.

At longer times the conversion rate decreases markedly and the reaction eventually reaches an equilibrium at conversion values close to 85%. As already mentioned the kinetics of the hydrolysis reaction can be equally monitored by following the absorbance decrease with time of the anhydride peak at 1066 cm^{-1} (see *Figure 2b*). In this case

$$\frac{\bar{A}_t^{1066}}{\bar{A}_0^{1066}} = \frac{[An]_t}{[An]_0}$$

and

$$f_{an}^t = \frac{\bar{A}_t^{1066}}{\bar{A}_0^{1066}} f_{an}^\circ$$

where the symbols have the usual meaning and

$$\bar{A}^{1066} = \int_{1025}^{1120} A \, dv$$

The value of f_{an}° (=0.84) is taken from the carbonyl region analysis of the spectrum at zero time.

The f_{an} values obtained in this way are reported as a function of exposure time in *Figure 3*, curve B. It is noted that the two determinations (curves A and B) coincide up to a value for f_{an} of 0.5. At lower values the determination arising from the 1066 cm^{-1} peak is slightly lower than that obtained from the carbonyl region. This effect could be associated with the significant degree of overlapping of the carbonyl absorptions relative to the anhydride and to the acid functionalities. The authors believe the former f_{an} evaluation to be slightly more accurate than the latter. In the system consisting of a thin EPR-g-SA film surrounded by a constant-humidity environment the hydrolysis of the anhydride units can occur according to two different mechanisms.

In the first mechanism the diffusion of H_2O across the film–environment interface controls the rate of reaction. This mechanism would yield the following zero-order rate equation[11]:

$$[An]_t = [An]_0 + Ct \qquad (1)$$

where $C = DA[H_2O]_w/VX$, D is the diffusion coefficient of water across the film–environment interface, A is the interfacial area, $[H_2O]_w$ is the water concentration in the environment, V is the volume of the film and X is the thickness of the interface.

In the second mechanism the water saturates the copolymer film and maintains a constant concentration due to rapid diffusion of water across the interface. The rate of reaction is controlled by the rate of hydrolysis within the bulk of the modified rubber.

This mechanism would yield the following pseudo-first-order rate equation[11]:

$$\ln \frac{[An]_t}{[An]_0} = K't \qquad (2)$$

where $K' = K[H_2O]_i$, K is the reaction rate constant, and $[H_2O]_i$ is the H_2O in the polymer film.

In *Figure 4* $[An]_t$ and $\ln([An]_t/[An]_0)$ are plotted

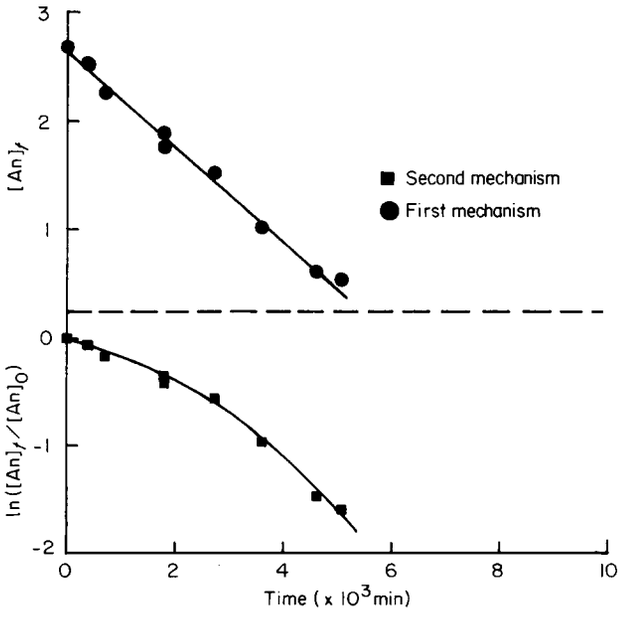

Figure 4 $[An]_t$ (●) and $\ln[An]_t/[An]_0$ (■) *versus* hydrolysis time

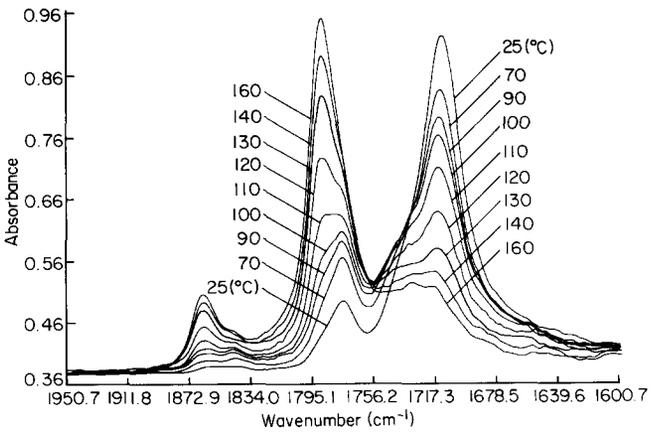

Figure 5 *FT*i.r. spectra in the range 1950–1600 cm^{-1} of EPR-g-SA at temperatures indicated (all spectra are reported in absolute absorbance scale)

against the exposure time, according to equations (1) and (2).

It is apparent that a linear trend is obtained only for the first mechanism (correlation coefficient exceeding 0.99), indicating that the hydrolysis rate is controlled by water diffusion. This conclusion is further confirmed by the observation that the thickness of the EPR-g-SA samples affects only the kinetics of the anhydride hydrolysis, but does not influence the final conversion values obtained at equilibrium.

The hydrolysis of anhydride groups is thermally reversible: in fact the succinic acid functionalities easily undergo thermal cyclization by losing a water molecule. Again the phenomenon can be suitably monitored by *FT*i.r. spectroscopy.

In *Figure 5* the spectra of the functionalized EPR in the 1920–1600 cm^{-1} interval, at temperatures ranging from 25°C to 160°C are shown. Each spectrum shown has been taken after 30 min of stabilization at the test temperature. It was checked that this time period is sufficiently long to reach equilibrium conditions. The anhydride doublet is observed to increase gradually with temperature at the expense of the succinic acid absorption at 1712 cm^{-1}. The parameter f_{an} has been evaluated as previously, assuming that the ratio $\varepsilon_{an}/\varepsilon_{ac}$ does not change markedly with temperature.

The f_{an} values as a function of temperature are reported in *Figure 6*: an S-shaped curve is obtained. Up to 50°C no significant cyclization of the acid moieties occurs; beyond this value f_{an} starts to increase substantially, reaching a final value of 0.75 at 150°C.

It has already been noted that in the hydrolysis experiment made at room temperature the anhydride $\nu_{as,C=O}$ peak at 1785 cm^{-1}, which is highly symmetrical when the amount of succinic acid groups is very low (see *Figure 2a* spectrum at time zero), develops an increasing asymmetry in the lower frequency side as the concentration of acid groups increases. Moreover, starting from an acid content of about 2.2%, the 1785 cm^{-1} anhydride peak is clearly split into a doublet (see *Figure 2a*, spectra at 4600, 5080, 6400 and 17 600 min). The two components of this doublet are not completely resolved, but their separation, as evaluated by second derivative analysis, is about 10 cm^{-1}.

A further interesting observation is that the relative intensity of the two components of the ν_{as} anhydride peak changes as a function of the acid content. In particular, the low-frequency component increases gradually, at the expense of the component at higher frequency and becomes predominant at an acid content of 2.2%.

These experimental observations can be explained in terms of hydrogen-bonding interactions involving the anhydride carbonyls as proton acceptors and the O–H groups of the succinic acid moieties, which function as proton donors.

It is in fact well known that such interactions cause a decrease in the force constant of the C=O double bonds, thus producing a shift of the relative infrared absorption towards lower wavenumbers. Generally no strong intensity effects are observed[12,13]. Thus at a sufficiently high concentration of the proton donor groups two different populations of anhydride moieties are present: those associated through a hydrogen-bonding interaction with the carboxylic groups and those that are free from any interaction. As the concentration of proton donors increases, the population of interacting anhydride groups obviously increases at the expense of the anhydride units that do not interact. This behaviour is even clearer in the temperature experiment. At 25°C, when the succinic anhydride groups are almost completely hydrolysed, the population of interacting anhydride groups is strongly predominant; in fact the relative peak is found at 1775 cm^{-1}, 10 cm^{-1} lower than the $\nu_{as,C=O}$ anhydride peak in the anhydrous state. As the temperature increases the succinic acid content decreases due to the cyclization reaction and the number of non-interacting anhydride groups grows accordingly. The populations of interacting and non-interacting anhydride units appear to be almost identical at 110°C while, for higher temperatures, the latter population becomes predominant. At 160°C the $\nu_{as,C=O}$ peak occurs again at 1785 cm^{-1} and is highly symmetrical, thus indicating the almost complete disappearance of the interacting anhydride units.

From geometrical considerations the authors have verified the possibility that a succinic acid group and an anhydride unit can be arranged so as to form two hydrogen-bonding interactions. The resulting structure

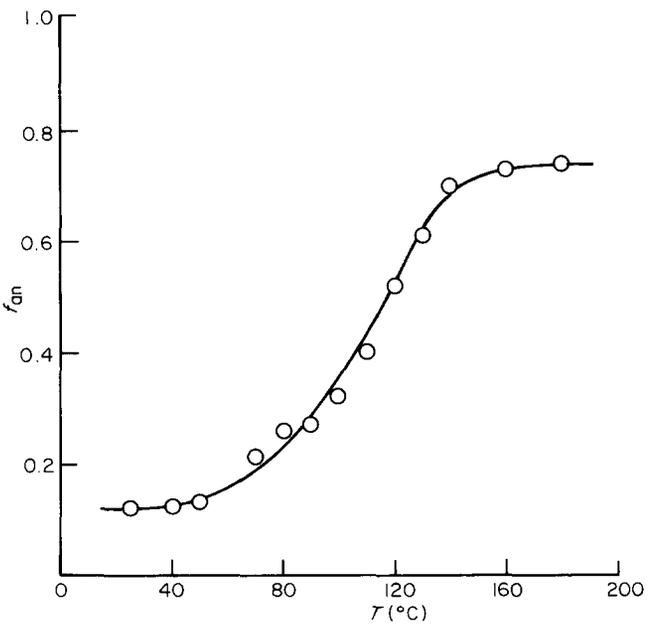

Figure 6 Fraction of anhydride groups (f_{an}) as a function of temperature for EPR-g-SA

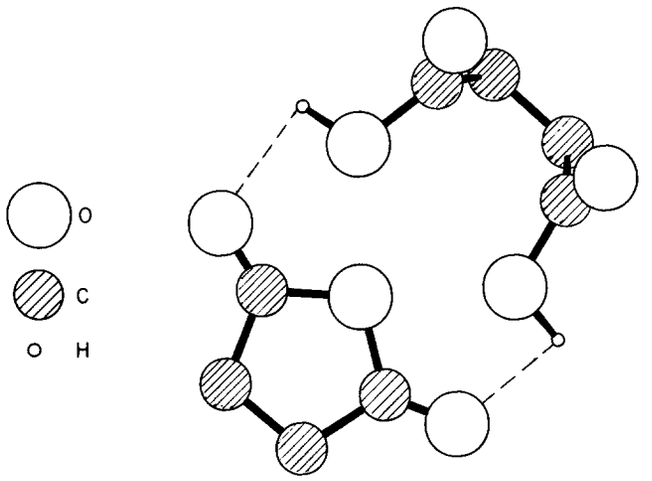

Figure 7 The structure of the hydrogen-bonding interaction between succinic acid and succinic anhydride groups

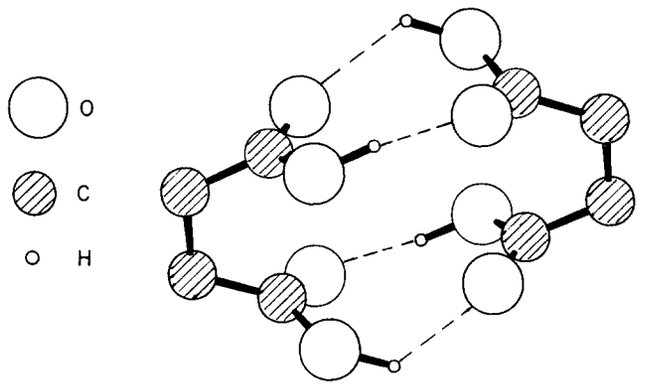

Figure 8 The structure of the hydrogen-bonding interaction between two succinic acid groups

of this adduct is represented in *Figure 7*. A preliminary analysis seems to suggest that the proposed structure is also consistent on the basis of energetic considerations. However, a more detailed conformational analysis is currently underway to obtain more definitive results about the structure of this hydrogen-bonding interaction.

The absorption relative to the C=O groups of the succinic acid also shows a complex pattern (see *Figure 2a*). In fact a highly symmetrical profile centred at 1712 cm^{-1} shows a clearly defined shoulder on the higher frequency side. Analogous considerations can therefore be applied: the shoulder at higher frequency can be attributed to the 'free' carbonyls of the succinic acid groups, while the peak at 1712 cm^{-1} is due to the self-interacting ones. It seems worth noting that the relative intensity of these two components indicates that the population of self-interacting carboxylic groups is always predominant, even at very low concentration. Furthermore, the highly symmetrical shape of the profile relative to the stretching mode of the interacting C=O groups seems to suggest the occurrence of a single, well defined type of hydrogen-bonding interaction among the carboxylic units.

As for the acid–anhydride interaction, the authors have verified the possibility that two succinic acid units can assume a conformation that allows the formation of the maximum number of hydrogen-bonding interactions. In *Figure 8* the resulting structure of this adduct is shown, in which four interactions are realized. Obviously structures with a minor number of interactions could be proposed.

In general if the absorptions of interacting and non-interacting groups were completely separated, the proportion of the groups involved in specific interactions could be calculated from the areas of the two separated components, provided that their relative absorptivities are known. In our case even though the perturbation of the $\nu_{C=O}$ absorption is significant, it is not sufficient to allow a reliable separation of the two components (see *Figure 9*, $T = 25°C$). However, an increase in resolution is expected if the infrared measurement is made at very low temperatures. This is because a general sharpening of the i.r. absorptions occurs at these temperatures and because, decreasing the interatomic distances, increases the hydrogen bonding strength and hence the perturbation of the carbonyl absorption.

These effects are indeed observed when the spectrum is collected at $-150°C$ (compare spectra at 25°C and at $-150°C$ in *Figure 9*). The main carbonyl peak, which is due to the interacting groups, shifts, at $-150°C$, from 1712 cm^{-1} to 1710 cm^{-1} and its full width at half height (FWHH) decreases from 29 cm^{-1} to 25 cm^{-1}. The higher frequency component (non-interacting carbonyls) remains hardly affected. The enhanced resolution of the low-temperature spectrum affords the complex spectral profile to be separated in the two original components by applying a curve-fitting algorithm based on a least-squares refinement procedure[14] (*Figure 10*). Finally, from the area of the peak at 1735 cm^{-1}, $\bar{A}_{1735}$ (11.4 cm^{-1}), and from that of the peak at 1709 cm^{-1}, $\bar{A}_{1709}$ (69.3 cm^{-1}), it is possible to evaluate the percentage of non-interacting carbonyls, α, by use of the relation

$$\alpha = \frac{\bar{A}_{1735}}{\bar{A}_{1735} + (\varepsilon_{1735}/\varepsilon_{1709})/\bar{A}_{1709}} \times 100 \qquad (3)$$

By analogy with literature data on systems where a similar type of hydrogen-bonding interaction takes place (ethylene–methacrylic acid copolymers)[15] it has been assumed that the ratio $\varepsilon_{1735}/\varepsilon_{1709}$ is equal to 1.6. On this basis α was evaluated as 9.3% of the total succinic acid groups present in the system.

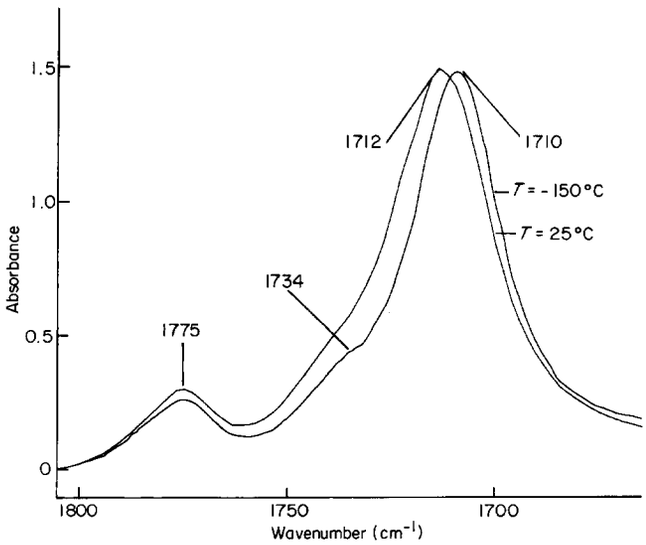

Figure 9 *FT*i.r. spectrum in the range 1800–1650 cm^{-1} of EPR-g-SA at ambient temperature and at $-150°C$

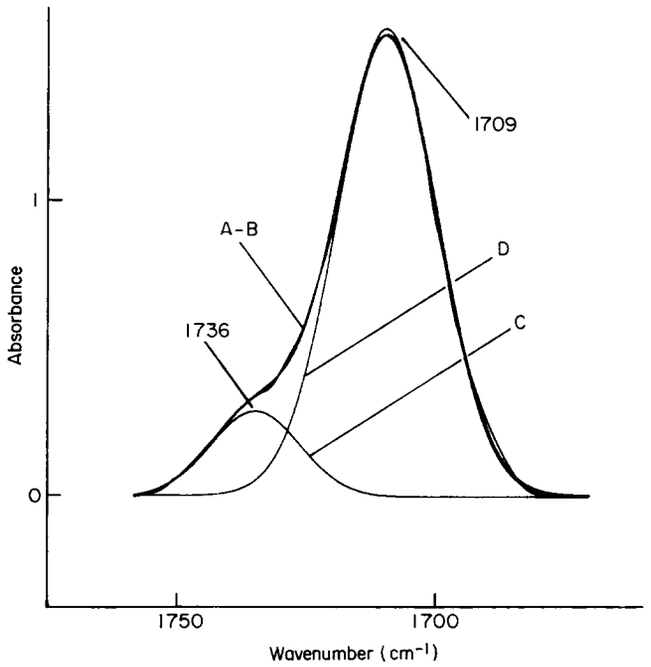

Figure 10 Curve fitting analysis of the carbonyl absorption of EPR-g-SA in the 1760–1650 cm^{-1} range. Spectrum collected at −150°C: (A) experimental spectrum; (B) best fitting of the experimental profile; (C) and (D) Gaussian components of spectrum (B)

Tensile mechanical behaviour. In order to evaluate the effects of the molecular interactions detected spectroscopically upon the mechanical properties of the modified rubbers, tensile mechanical measurements have been made. Nominal stress–strain curves obtained at ambient temperature and at a strain rate of $3.0 \times 10^{-3}\ s^{-1}$ are reported in *Figure 11*. The curves refer to the unmodified EPR, curve A, the anhydrous EPR-g-SA with a grafting degree of 3.0 wt%, curve B, and the same EPR-g-SA hydrolysed for 7 days at 25°C and at 60% relative humidity, curve C.

It was checked by *FT*i.r. that, in these conditions, the hydrolysis proceeds up to a conversion of 85% anhydride groups. Plain EPR shows the typical behaviour of an uncross-linked rubber. In fact at strain exceeding 50%, a steady flow regime is established, which continues up to rupture, occurring at about 400% deformation. Conversely, curve B exhibits a trend quite similar to that of a lightly cross-linked elastomer. Such behaviour is in agreement with spectroscopic evidence indicating that, in this case, only a small number of hydrogen-bonding interactions, which can act as cross-linking points, is present in the system. These interactions are due to the fact that, even in anhydrous conditions, about 15% of the total anhydride groups are hydrolysed and the succinic acid units so formed are able to self-associate even if their concentration is very low.

Curve C resembles the behaviour of a highly cross-linked rubber: the stress increases continuously with strain up to about 800% deformation; above this value an increase in the slope of the stress–strain curve is also observed. This trend can be related again to the increased number of hydrogen-bonding interactions. In this case, in fact, the grafted functionalities are mainly succinic acid groups, which interact both with themselves and with the remaining anhydride moieties.

Figure 12 shows the effect of the grafting degree of the functionalized rubber on the stress–strain behaviour. The four curves refer to plain EPR (curve A) and to modified EPRs having grafting degrees equal to 1.2, 3.0 and 4.4% by weight (curves B, C and D, respectively). Before testing, the modified rubber samples were fully hydrolysed as previously described.

The stress–strain behaviour of the samples investigated indicates an increase in cross-linking density with increasing degree of grafting. The same arguments used to explain the differences among anhydrous and hydrolysed EPR-g-SA also apply in the present case.

A further interesting observation is that the C and D curves display a marked increase in the slope at about 800 and 1000% deformation, respectively. In our opinion this effect can be related to an increase in cross-linking density that occurs during the deformation process, starting from a critical value of strain. Such an increase could be due to the formation of new hydrogen-bonding interactions among the succinic acid functionalities, which are still free in the undeformed state. In fact the 'free' carboxyl groups, which are occluded within the random coils of the EPR chains, can be rendered available to interact when the chains become highly extended. Recall that, from spectroscopic analysis, the concentration of such non-interacting groups was 9.2%

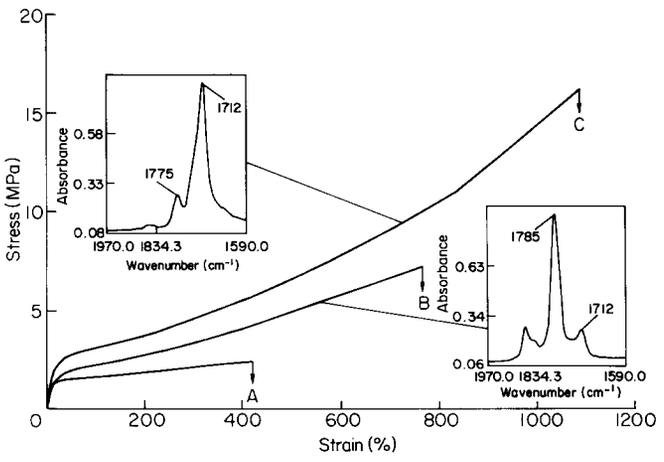

Figure 11 Stress–strain curves at ambient temperature for plain EPR (curve A), EPR-g-SA with a *DG* of 3 wt%, anhydrous (curve B) and the same EPR-g-SA fully hydrolysed (curve C) (the insets refer to the *FT*i.r. spectra in the range 1970–1590 cm^{-1} of the two EPR-g-SA samples)

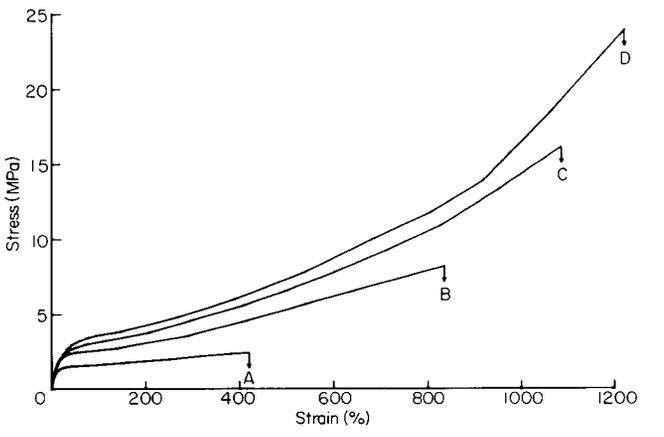

Figure 12 Stress–strain curves at ambient temperature for plain EPR (curve A) and EPR-g-SA with different grafting degrees: curves B, C and D refer to *DG* equal to 1.2, 3.0 and 4.4 wt%, respectively

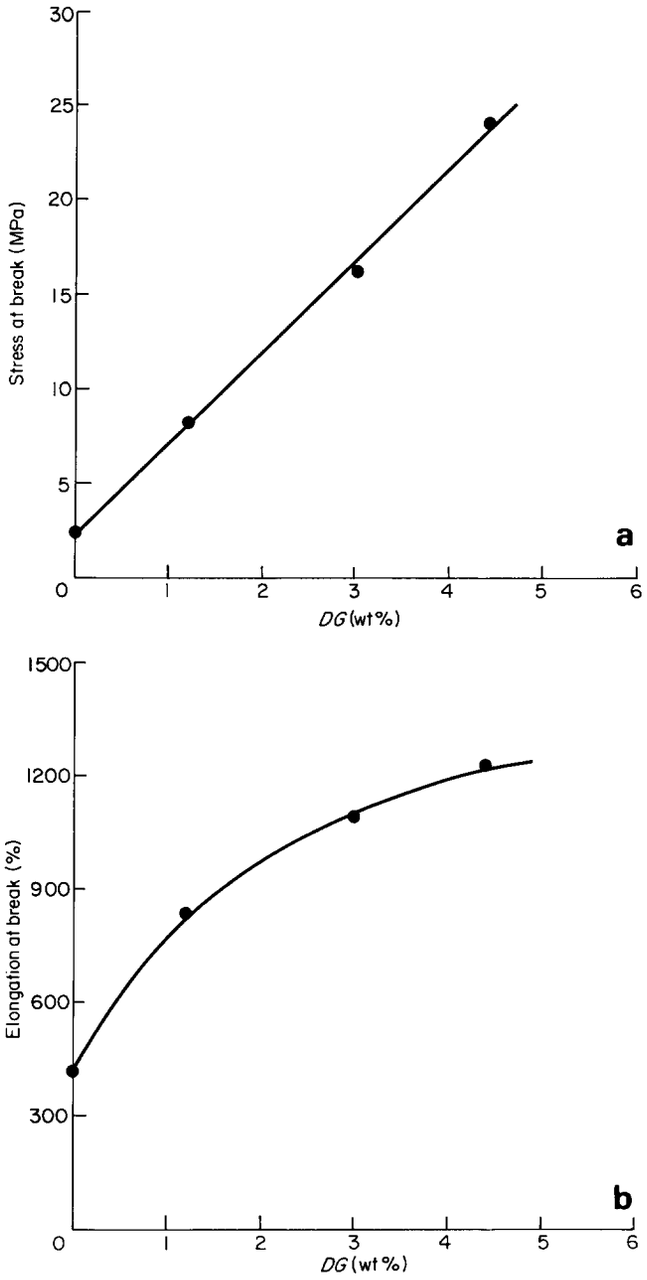

Figure 13 Stress at break (a) and elongation at break (b) as a function of *DG*

of the total succinic acid content in the EPR-g-SA sample with a degree of grafting of 3.0 wt%.

The ultimate properties such as stress (σ_B) and deformation (ε_B) at break of the four elastomers investigated are reported in *Figure 13a* and *b* as a function of the degree of grafting (*DG*). As can be expected on the basis of the above considerations, both these parameters increase with increasing *DG*; in particular σ_B exhibits a linear trend.

Application of functionalized rubbers in PA6-based blends

Among the various applications of EPR rubbers functionalized by succinic anhydride, of particular interest is their use as toughening agents in thermoplastic matrices such as PA6 and poly(butadiene/terephthalate) (PBT)[16,17]. In particular the effectiveness of an EPR-g-SA copolymer in improving the toughness of both PA6 and PBT has been demonstrated[6,7].

In previous investigations the EPR copolymer had a composition of 50 mol% C_2 units and a residual crystallinity lower than 2.0 wt%. In the present study the EPR used had a higher C_2 content (78 mol%) and higher values of residual crystallinity (*ca.* 10%). The mechanical and impact properties of PA6/EPR-g-SA blends at a fixed composition (80/20% by weight) have been measured.

The role of the *DG* of the modified elastomer on the above properties has been investigated as well. In *Figure 14* the stress–strain diagrams obtained at room temperature and at a strain rate of $3.0 \times 10^{-3}\ s^{-1}$ for plain PA6 (curve A) and for three PA6/EPR blends where the EPR copolymer has a *DG* equal to 0, 3.0 and 4.4 wt% (curves B, C and D, respectively) are shown. Tensile parameters calculated from the diagrams, such as Young's modulus (E), stress (σ_B) and deformation (ε_B) at break are summarized in *Table 1*. It can be noted that the overall effect of the rubber addition on the PA6 tensile behaviour is a reduction of E, ε_B and σ_B. The lowering of E and σ_B is hardly influenced by the nature of the rubber as well as by its *DG*.

On the contrary, the values of ε_B are observed to increase gradually with increasing *DG*. This result can be interpreted on the basis of the morphological analysis performed on cryogenically fractured surfaces, which were successively etched by xylene vapours. From the SEM micrographs of these surfaces it can be seen that for the PA6/EPR blend (*Figure 15a*) the rubber is segregated in spherically shaped domains regularly distributed throughout the samples. The dimensions of such domains are quite large: the diameter ranges from 5 to 20 μm. The walls of the cavities seem to be very smooth, indicating no adhesion between the matrix and the rubber.

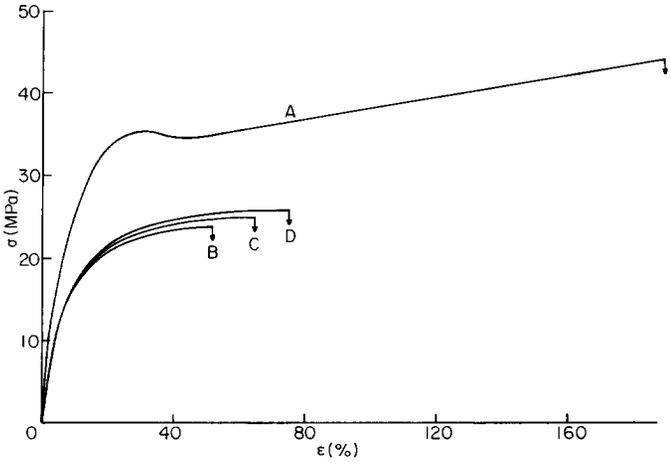

Figure 14 Stress–strain curves for plain PA6 (curve A) and for PA6/EPR-g-SA blends with a *DG* of the rubber equal to 0 (curve B), 3.0 (curve C) and 4.4 wt% (curve D)

Table 1 Modulus (E), stress (σ_B) and elongation (ε_B) at break for PA6 homopolymer and for PA6 rubber blends

Sample	*DG* (wt%)	E (GPa)	σ_B (MPa)	ε_B (%)
PA6	–	0.6	44	200
PA6/EPR	0	0.35	24	53
PA6/EPR-g-SA	3.0	0.33	25	65
PA6/EPR-g-SA	4.4	0.36	26	75

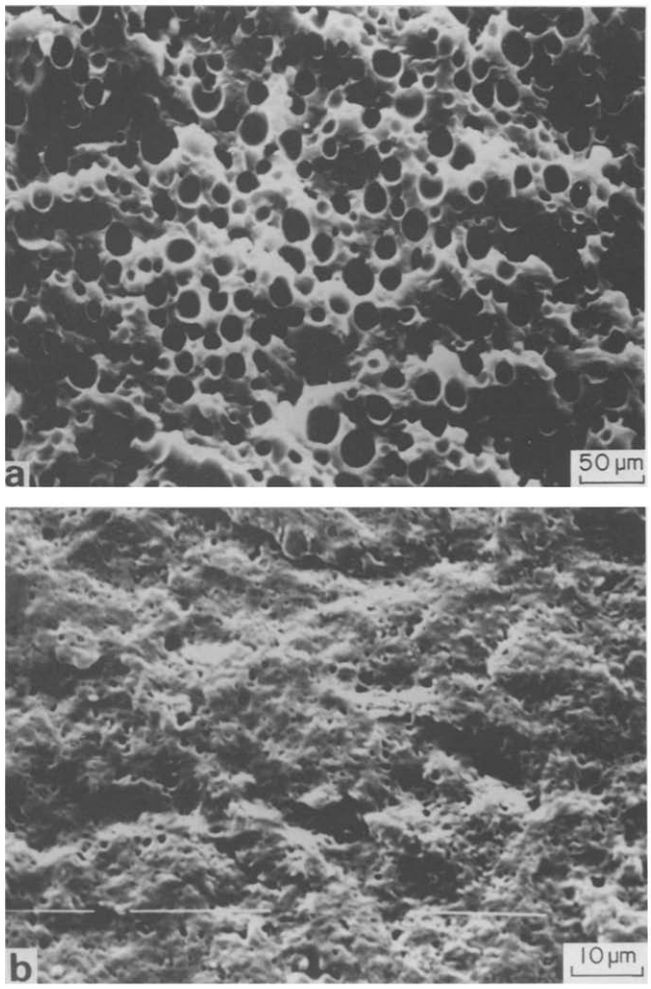

Figure 15 Scanning electron micrographs of cryogenically fractured and etched surfaces of PA6/EPR (a) and PA6/EPR-g-SA with a *DG* of 3.0 wt% (b)

For the PA6/EPR-g-SA blend with a *DG* for the rubber equal to 3.0% (*Figure 15b*), the dimension of the rubber particles is strongly reduced. The diameter of the holes is less than 1 μm. Furthermore, the amount of material etched seems to be smaller than in the former case. Such an observation may be related to the presence of an (EPR-g-SA)-g-PA6 graft copolymer formed during the mixing process, which can act as compatibilizing agent. The PA6 branches of such a copolymer are firmly fixed into the PA6 matrix, rendering the rubbery dispersed phase less extractable by the solvent. For the PA6/EPR-g-SA blend with a *DG* of the rubber equal to 4.4%, the overall morphological features remain unchanged. This indicates that once a critical domain size is obtained, an increase of the *DG* of the modified rubber does not affect this morphological parameter. However, an increase of adhesion among the two phases can be expected by increasing *DG*, since a higher concentration of the (EPR-g-SA)-g-PA6 graft copolymer is formed.

The very low ε_B value observed in the case of the PA6/EPR blend can be attributed essentially to the presence of the large EPR particles with poor adhesion to the matrix. Such domains act as gross material defects, causing a premature rupture of the specimen soon after the beginning of the yielding process.

For the two PA6/EPR-g-SA blends the finer dispersion of the rubbery phase with improved adhesion to the matrix induces local yielding of PA6 around the rubber particles, enhancing the capability of the material to be plastically deformed. This deformation mechanism is more effective at higher *DG* values, possibly because of increased adhesion among the phases.

The impact properties of the blends investigated as a function of testing temperatures are shown in *Figure 16*. For the PA6 homopolymer, curve A, the impact resistance (I) is very low and its value remains constant over the whole temperature range investigated. A similar behaviour is observed for the blend containing unmodified EPR, curve B. For the blends containing EPR-g-SA as rubbery phase, a large enhancement of I is found with respect to pure PA6, curves C and D. From the trend of the curves it emerges that I increases with enhancing *DG* of EPR-g-SA. Furthermore the two blends containing the modified rubber display a marked transition from a brittle to a ductile mode of failure. The temperature at which such a transition occurs depends on *DG*: it decreases with increasing *DG*.

Figure 17 shows SEM micrographs of the surfaces obtained after impact failure at ambient temperature of (*a*) PA6/EPR and (*b*) PA6/EPR-g-SA with *DG* of 3.0%. These pictures have been taken near the notch tip in the region of crack initiation.

From *Figure 17a* it appears that a large number of rubber particles are pulled away during the fracture process, again indicating poor adhesion at the PA6–rubber interface. Moreover no evidence of localized plastic deformations (crazes and/or shear bands) are visible, thus explaining the low values of fracture toughness observed.

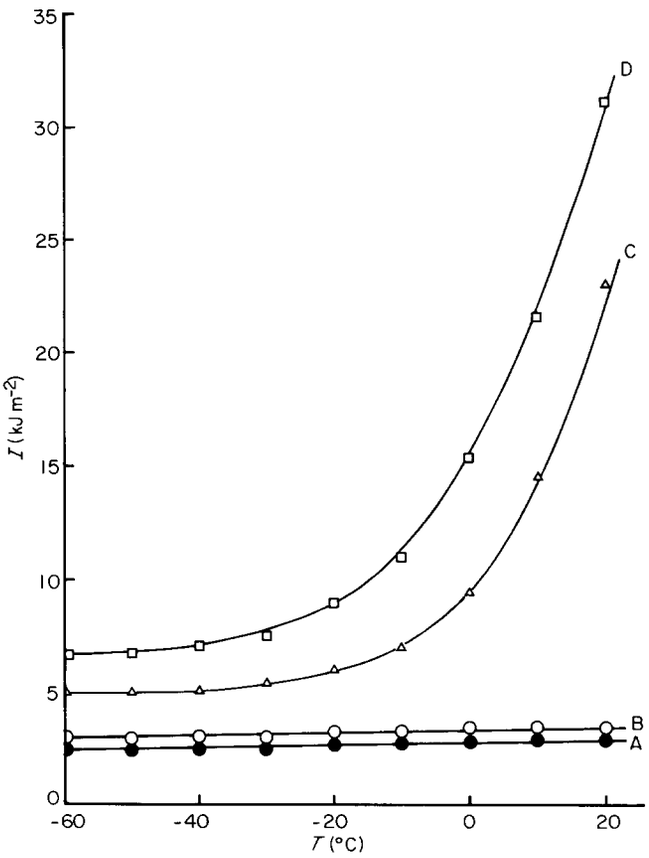

Figure 16 Impact strength *versus* temperature for PA6 (curve A), PA6/EPR (curve B), and PA6/EPR-g-SA with a *DG* of the rubber equal to 30 (curve C) and to 4.4 wt% (curve D)

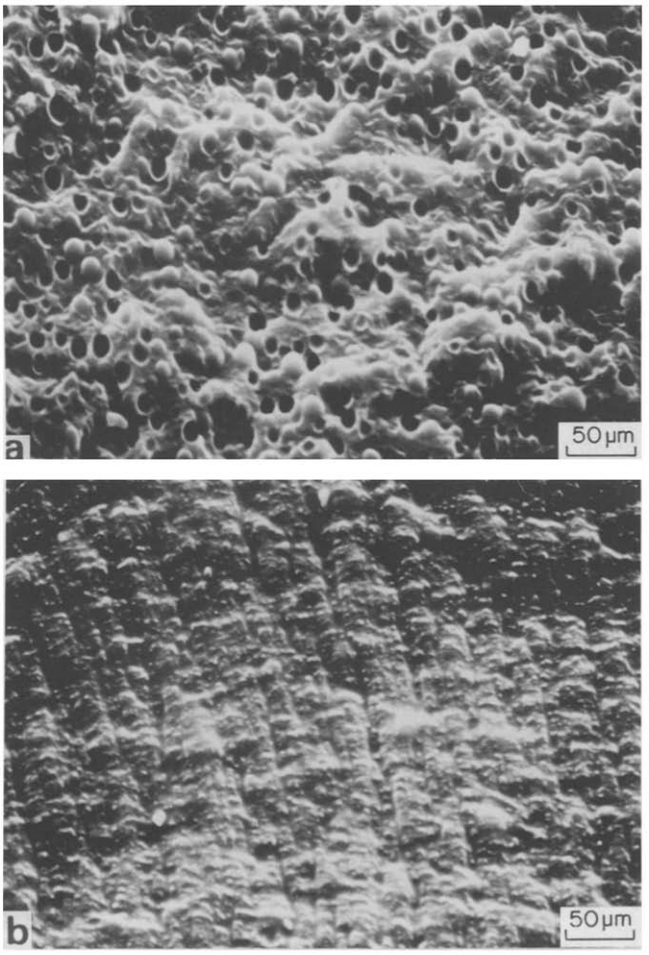

Figure 17 Scanning electron micrographs of PA6/EPR (a) and PA6/EPR-g-SA, $DG = 3.0$ wt% (b): surfaces fractured at ambient temperature by the Charpy test

In the blends containing EPR-g-SA as rubbery component the morphology of the fractured surface appears to be completely different (compare *Figure 17a* and *b*). In this case development of bands or of rumpling is evident. This suggests that a large amount of plastic deformation occurs during the fracture process. Such ductile behaviour is due to matrix shear yielding induced by the presence of finely dispersed and well-bonded rubber particles[18,19].

CONCLUSIONS

A study of an ethylene–propylene copolymer functionalized by succinic anhydride groups has been made by using various characterization techniques. In particular *FT*i.r. spectroscopy has been used to investigate the hydrolysis of the anhydride functionality at room temperature. The cyclization reaction of grafted succinic acid groups at various reaction temperatures has also been analysed. The nature of the molecular interactions occurring in such modified elastomers has been studied by the same spectroscopic technique. Hydrogen-bonding interactions between carboxylic acid units and between carboxylic acid and anhydride groups have been identified. An evaluation of the COOH groups not involved in such interactions at room temperature and in the fully hydrolysed state was also made.

The mechanical tensile behaviour of EPR-g-SA has been investigated and interpreted in terms of the molecular interactions identified spectroscopically. It has been found that the mechanical response of such materials improves markedly with increasing the number of hydrogen bonds present in the system.

The possibility of improving the mechanical and the impact properties of PA6 by the addition of EPR-g-SA has also been confirmed. The effectiveness of EPR-g-SA as a toughening agent has been found to increase by increasing the degree of grafting. A comparison with previously reported data suggests that the composition of the EPR copolymer does not influence its role as toughening agent.

ACKNOWLEDGEMENTS

Thanks are due to Mr A. Lahoz and Mr L. Serio for technical assistance.

This paper has been partly supported by 'Progetto Finalizzato Chimica Fine II' of the Italian C.N.R.

REFERENCES

1 Minoura, Y., Veda, M., Minozuma, S. and Oba, M. *J. Appl. Polym. Sci.* 1969, **13**, 1625
2 De Vito, G., Maglio, G., Lanzetta, N., Malinconico, M., Musto, P. and Palumbo, R. *J. Polym. Sci., Polym. Chem. Edn.* 1984, **22**, 1334
3 Gaylord, N. G. and Mishra, M. *J. Polym. Sci., Polym. Lett. Edn.* 1983, **21**, 23
4 Greco, R., Maglio, G. and Musto, P. *J. Appl. Polym. Sci.* 1989, **33**, 789
5 Cimmino, S., D'Orazio, L., Greco, R., Maglio, G., Malinconico, M., Mancarella, M., Martuscelli, E., Palumbo, R. and Ragosta, G. *Polym. Eng. Sci.* 1984, **24**, 48
6 Greco, R., Malinconico, M., Martuscelli, E., Ragosta, G. and Scarinzi, G. *Polymer* 1987, **28**, 1185
7 Cecere, A., Greco, R., Ragosta, G., Scarinzi, G. and Taglialatela, A. *Polymer* 1990, **31**, 1239
8 Bellamy, L. J. 'The Infrared Spectra of Complex Molecules', Vols I and II, Chapman and Hall, London, 1980
9 Colthup, N., Daly, L. and Wiberley, S. 'Introduction to Infrared and Raman Spectroscopy', Academic Press, New York, 1975
10 Saier, E. L., Petrakis, L., Cousins, L. R., Heilman, W. J. and Hezel, J. F. *J. Appl. Polym. Sci.* 1968, **12**, 2191
11 Frost, A. A. and Pearson, A. 'Kinetics and Mechanism', John Wiley & Sons, New York, 1961
12 Pimentel, G. C. and McChellan, A. L. 'The Hydrogen Bond', Freeman, San Francisco, 1960
13 Vinograda, S. N. and Linnell, R. H. 'Hydrogen Bonding', Van Nostrand Reinhold, New York, 1971
14 Maddams, W. F. *Appl. Spectrosc.* 1979, **34**, 245
15 Lee, J. Y., Painter, P. C. and Coleman, M. M. *Macromolecules* 1988, **21**, 346
16 Greco, R., Malinconico, M., Martuscelli, E., Ragosta, G. and Scarinzi, G. *Polymer* 1988, **29**, 1418
17 Cimmino, S., Coppola, F., D'Orazio, L., Greco, R., Maglio, G., Malinconico, M., Mancarella, C., Martuscelli, E. and Ragosta, G. *Polymer* 1986, **27**, 1875
18 Speroni, F., Castaldi, E., Fabbri, P. and Casiraghi, T. *J. Mater. Sci.* 1989, **24**, 2165
19 Immirzi, B., Laurienzo, P., Malinconico, M. and Martuscelli, E. *J. Polym. Sci., Polym. Chem. Edn.* 1989, **27**, 829